

Optimization of Malachite Green Dye Removal Efficiency via Factorial Design Analysis Using Metal-Organic Frameworks

Renuka Garg¹, Rana Sabouni^{1*} Abdulwahab Alaamer¹, Aysha Alali¹, Dana Al-Muqbel¹, Hind Alqassem¹ and Khawla Almazrooei¹

¹Department of Chemical and Biological Engineering, American University of Sharjah, Sharjah, United Arab Emirates
renuka940@gmail.com, rsabouni@aus.edu

*Corresponding Author: Rana Sabouni, PhD, Department of Chemical and Biological Engineering, American University of Sharjah, Sharjah, United Arab Emirates

Abstract - In this study, we investigate the adsorption of the cationic dye Malachite Green (MG) onto two metal-organic frameworks, ZIF-8 and Fe-BTC. We effectively prepared beads using a polymer coating process with sodium alginate. To study the effect of different factors on adsorption capacity and removal %age of Malachite Green in a batch process, we employed a 2³ factorial design study analysis. The investigation involved three primary factors, each with two levels: MOF type (A: Fe-BTC and ZIF-8), MOF bead dosage (B: 50 mg to 100 mg), and initial concentration (C: 5 mg/L to 17 mg/L). The primary effects of these variables and their interactions were examined using Response Surface Methodology (RSM), main effect, interaction effect, and Pareto chart. The factorial design analysis, conducted using analysis of variance (ANOVA), revealed that the most significant factor influencing adsorption capacity was the initial concentration of MG, followed by the dosage of MOF beads and the type of MOFs. The study demonstrates that SA@ZIF-8 beads have achieved the highest removal rate of 96%, in comparison to SA@Fe-BTC which reaches 90%. Notably, the initial concentration of MG demonstrates a positive effect, MOF dosage exhibits a negative effect, while the MOF type presents a positive effect, favoring SA@ZIF-8 for higher adsorption capacity. Moreover, significant two-way and three-way interactions were identified. The optimum conditions for the maximum removal of MG dye using SA@ZIF-8 were reported as follows: adsorbent dosage = 50 mg; MG initial concentration = 17 mg/L. The R² value > 98.8% for MG dye underscores the potency of the factorial design model, thereby encouraging further exploration and application of SA@ZIF-8 metal-organic framework to eliminate pollutants from aqueous solutions.

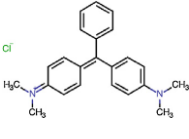
Keywords: Metal-organic frameworks; Beads; Adsorption; Malachite green; Factorial design

© Copyright 2024 Authors - This is an Open Access article published under the Creative Commons Attribution License terms (<http://creativecommons.org/licenses/by/3.0>). Unrestricted use, distribution, and reproduction in any medium are permitted, provided the original work is properly cited.

1. Introduction

The textile industry is a significant contributor to industrial water pollution, responsible for approximately 17–20% of the total industrial water pollution in aquatic systems [1]. The alarming release of hazardous chemicals into the environment is a pressing concern, especially with the rapid growth of the textile industry. Among these pollutants, Malachite Green is particularly concerning due to its widespread use and potential for harm. Malachite Green is a cationic dye in the triphenylmethane class, recognized for its vibrant colour and versatility in various industrial applications. [2]. The properties and structure of the Malachite Green dye are provided in Table 1. MG dye finds extensive use in dyeing silk, cotton, paper, and leather products. Despite its common application, Malachite Green poses significant health risks, being both mutagenic and carcinogenic [3], [4]. Exposure to this dye can lead to acute adverse effects on vital organs such as the kidney, liver, and nervous system [5]. Even at low concentrations, Malachite Green can result in significant consequences, such as colouring large bodies of water, which can impede photosynthesis by obstructing light penetration. Consequently, this disruption prevents the growth of marine life, highlighting the environmental hazards associated with its use.

Table 1: Characteristics of Malachite green dye

| | | | |
|------------------------------------------------------|---------------------|---------------------------|-----------------------------------------------------------------------------------|
| Generic Name | Malachite Green | Type of dye | Cationic |
| Chemical Formula | $C_{23}H_{25}ClN_2$ | $\lambda_{max}(nm)$ | 624 |
| Molecular Weight ($\frac{g}{mol}$) | 364.91 | Chemical structure |  |

Existing methods like ion exchange, coagulation, filtration, advanced oxidation, biodegradation, and ultrafiltration effectively remove pollutants from water but face challenges of cost and contamination [6], [7]. In contrast, adsorption stands out for its simplicity, affordability, and regenerative capabilities. Yet, conventional adsorbents are costly and have limited capacity, highlighting the urgent need for affordable dye removal in wastewater. Developing eco-friendly and cost-effective wastewater treatment techniques is crucial, enabling the reuse of treated water in regions lacking access to pure water resources. This advancement could provide a viable solution in areas with limited water access, promoting sustainable practices and environmental preservation.

Metal-organic frameworks (MOFs) are renowned for their intricate structures and versatile applications in separating and adsorbing various molecules [8], [9]. Among these MOFs, iron 1,3,5-benzenetricarboxylate (Fe-BTC) has proven effective in liquid-phase separation, demonstrating its versatility across different compounds [7], [10]. Similarly, the 2-methylimidazole zinc salt (ZIF-8) has gained attention for its remarkable attributes, including high thermal stability and exceptional chemical resistance during liquid-phase adsorption [11]. For the removal of Rhodamine B dye from water, Nazir and his team synthesized a nanocomposite derived from ZIF-8 and ZIF-67. They found that the composite had higher adsorption capacity ($Q_e=35.93 \text{ mg g}^{-1}$) at a basic pH of 10 compared to an acidic pH of 2 ($Q_e=12.81 \text{ mg g}^{-1}$) [12]. Moreover, it was found that a polymer-coated MOF approach enhanced the stability of MOFs in acidic environments.

Leveraging these unique properties, our present research focuses on utilizing ZIF-8 and Fe-BTC MOFs beads for removing hazardous dyes from aqueous

streams. We will utilize "design of experiment" (DOE) analysis to identify the optimal conditions for dye adsorption onto Metal-Organic Frameworks (MOFs). To achieve this, we employed a well-established MOF/Malachite blue (MG) system as a model. Using a 2^3 factorial design, we explored the impact of three key factors: (1) the type of MOF, (2) the dosage, and (3) the initial concentration on the efficiency of the adsorption process. Specifically, we studied commercially available MOFs, Basolite® F300 (Fe-BTC) and Z1200 (ZIF-8), for the adsorption of azo cationic MG dye from aqueous solutions. Our analysis aimed to optimize the MOF-based adsorption process for enhanced efficiency and practical applicability in various industrial effluent treatments. This approach showcases the innovative solutions MOFs offer for addressing challenges in separation and adsorption processes.

2. Materials and Methods

2.1 Materials

Fe-BTC and ZIF-8 were obtained from Sigma-Aldrich under the Basolite® F300 and Basolite® Z1200 trademarks. Malachite Green (MG) was purchased from LabChem (USA). Aqueous solutions of 1M HCl and NaOH, prepared from hydrochloric acid of 37% and sodium hydroxide, and were used for pH adjustments. Sodium alginate (>95%) and ethanol were obtained from Sigma-Aldrich Co., USA. Calcium chloride (> 97%) was used without further purification.

2.2 Characterizations

The characterization of the MOF samples was conducted through various analyses. The functional groups in the MOF samples were studied by recording Fourier Transform Infrared (FTIR) spectra with a PerkinElmer FTIR instrument (USA). Additionally, the shapes and morphologies of the MOF samples were examined using Scanning Electron Microscopy (SEM). The surface area and pore size were measured through Brunauer-Emmett-Teller (BET) analysis. Furthermore, UV-2600 Shimadzu spectrometer was used to measure the dye concentration, providing valuable insights into the properties of the MOF samples.

2.3 Adsorption Experiments

In the adsorption experiments, 50-100 mg of MOF was introduced into 50 mL of a 5-20 mg/L MG solution at a pH of 6 and room temperature (25 °C). The mixtures were vigorously stirred using a magnetic stirrer in a sealed beaker, and samples were extracted after specific time intervals (ranging from 5 to 120 minutes). The

adsorption process was carried out by collecting 5 mL samples at regular 5-minute intervals for UV measurements until equilibrium was achieved. The absorbance of the MG dye solution was measured both before and after adsorption at its maximum wavelength of 624 nm.

The amount of adsorbed MG per unit mass of MOF (qt) at any time (t) was calculated using equation (1).

$$q_t = (C_o - C_t) \times \frac{V}{m} \quad (1)$$

where C_o , C_t , V , m is the initial MG concentration, the MG concentration at time t , the MG solution's volume, and the MOF's dosage, respectively. In addition, equation (2) was used to calculate removal efficiency (RE).

$$RE = \frac{(C_o - C_t)}{C_o} \times 100 \quad (2)$$

Where initial concentration (mg/L) is denoted as C_o , equilibrium concentration (mg/L) at time t is C_t .

2.4 Synthesis of adsorbent beads

To produce SA@ZIF-8 and SA@Fe-BTC MOF composites, 0.2 g of ZIF-8 and Fe-BTC were first dissolved separately in deionized water [5]. SA was dissolved in water until a thick solution was formed. Subsequently, the ZIF-8 and Fe-BTC solutions were stirred into the sodium alginate mixture overnight to achieve uniformly dispersed MOFs and SA solutions. The suspension was then dispensed through a syringe (14-inch gauge size) into a beaker containing a 0.1% (w/v) calcium chloride solution to form beads and left in the solution for 24 hours. The beads were subsequently washed several times with DI water and left to dry at room temperature for 48 hours.

3. Characterizations

3.1 FTIR

In the sodium alginate FTIR spectra, the hydroxyl group (-OH) peak appeared at 3340 cm^{-1} , while the asymmetric and symmetric stretching vibrations of the carboxyl group were observed at 1594 cm^{-1} and 1407 cm^{-1} , respectively (Figure 1a). C-O stretching vibrations were represented by the peak at 1025.2 cm^{-1} , and broad peaks between $3800 - 3000\text{ cm}^{-1}$ indicated the presence of hydroxyl groups in adsorbed water molecules. For the SA@Fe-BTC sample, peaks at 711.6 cm^{-1} , 760.5 cm^{-1} , 1380 cm^{-1} , 1448 cm^{-1} , 1577 cm^{-1} , and 1627 cm^{-1} were identified, indicating carboxylic (-COO-) asymmetric and symmetric stretching vibrations, (C-O) from the BTC ligand, and Fe-O bond vibrations [13], [14]. In the FTIR spectrum of SA@ZIF-8 beads, O-H vibrations of alginate were seen at 3140 cm^{-1} , with stretching vibrations of aliphatic C-H at 2910 cm^{-1} . Additionally, C-O stretching

modes were evident around 1026 cm^{-1} and 1100 cm^{-1} and bending vibrations of single bond -CH₃ bonds appeared near 1310 cm^{-1} and 1425 cm^{-1} [15].

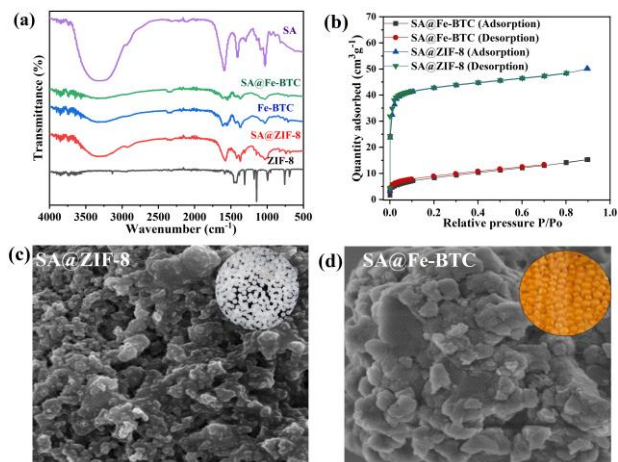


Figure 1: (a) FTIR spectra (b) BET analysis (c) SEM images of SA@ZIF-8 (d) SEM image of SA@Fe-BTC beads.

3.2 BET and SEM

The surface area of SA@ZIF-8 and SA@Fe-BTC beads was determined through N₂ adsorption-desorption experiments, as illustrated in Figure 1b. SA@ZIF-8 beads exhibited a BET surface area of $168.75\text{ m}^2/\text{g}$ and a pore volume of $0.069\text{ cm}^3/\text{g}$. In contrast, SA@Fe-BTC had a surface area of $30\text{ m}^2/\text{g}$ and a pore volume of $0.022\text{ cm}^3/\text{g}$ (Figure 1b). The addition of sodium alginate with ZIF-8 led to the formation of SA@ZIF-8 beads characterized by rough, porous surfaces and irregular cubical particles, as shown in. In comparison, the SEM image of SA@Fe-BTC displayed the existence of large crystals measuring 100 nm , composed of smaller crystals ranging from 10 to 20 nm . Additionally, the orange colour of the beads indicated the presence of iron as shown in Figure 1c and d.

3.3 Removal Efficiencies

Figure 2 presents a comparison of the adsorption capacities of two different adsorbents, namely SA@ZIF-8 and SA@Fe-BTC, under various conditions. The adsorption capacity of these MOFs was tested for MG (Malachite green) at different dosages and pollutant concentrations. At a dose of 50 mg and a pollutant concentration of 5 mg/L , SA@ZIF-8 exhibited the highest adsorption capacity for MG (Figure 2a). However, as the dose was increased from 50 mg to 100 mg , the adsorption capacity decreased. This decrease can be attributed to the hindrance of active sites due to the higher dose, which limits the adsorption efficiency. Furthermore, as the pollutant concentration was

increased from 5 mg/L to 17 mg/L, adsorption capacity increased for both SA@ZIF-8 and SA@Fe-BTC. Remarkably, at a dose of 50 mg, SA@ZIF-8 demonstrated the highest adsorption capacity of 8.06 mg/g in comparison to SA@Fe-BTC (3.49 mg/g) as shown in Figure 2b. This finding indicates that SA@ZIF-8 is more effective for MG dye adsorption compared to the SA@Fe-BTC catalyst beads. This can be attributed to the enhanced surface area of SA@ZIF-8 beads. SA@ZIF-8 showed promising performance at a dose of 50 mg and a pollutant concentration of 17 mg/L, which makes it a potential candidate for dye removal in practical applications.

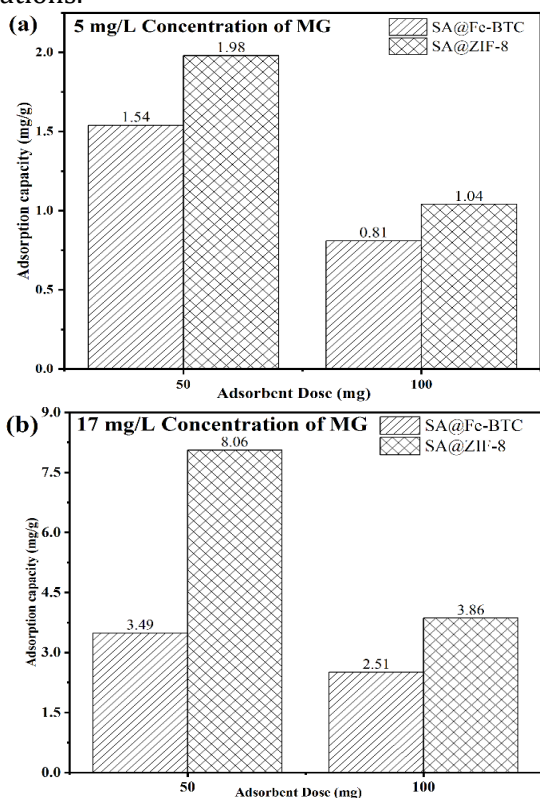


Figure 2: Adsorption Capacities SA@ZIF-8 and SA@Fe-BTC for Malachite Green (MG) at Varied Dosages and Pollutant Concentrations (a) 5 mg/L MG Concentration (b) 17 mg/L MG Concentration.

4. Factorial Design Analysis

A factorial design was utilized to explore the simultaneous impact of multiple factors on the adsorption process. This method allows the alteration of all variables such as adsorbent dosage, initial concentrations of MG, and their interactions, to determine the overall response. The experimental results indicate that the adsorption capacity of both SA@ZIF-8 and SA@Fe-BTC is influenced by the dosage of

the adsorbents and the concentration of the pollutant in the solution. Therefore, the study will focus on the main experimental factors. Specifically, a 2^3 factorial design was developed, investigating the influence of three key factors: MOF type (A) (Fe-BTC - ZIF-8), MOF dosage (B) (50 - 100 mg), and initial concentration (C) (5 - 17 mg/L) at two levels each, with experiments replicated twice. Further the standard deviation (STD) was calculated based on repeated values of % removal and found to be in range of 0.28-3.8 indicating consistent and reliable results (Table 2). The complete factorial experimental design, generated and randomized using Minitab software, is outlined in Table 2.

To plan and analyse this factorial design, Minitab 17.1.0 statistical software was utilized. This software played a vital role in exploring variable interactions and identifying the primary impacts of dye adsorption at a confidence level exceeding 95%. A total of 16 experiments were conducted based on the factorial design, providing malachite green adsorption capacity and removal efficiency (Table 3). In this design, the signs (positive or negative) denoted high and low levels, respectively, for each variable. For example, a positive sign for MOF indicated the use of SA@ZIF-8, while a negative sign represented the use of SA@Fe-BTC.

Table 2: The factors and their corresponding levels used in the factorial design.

| Factor | Code | Low Level (-1) | High Level (+1) |
|------------------------------|------|----------------|-----------------|
| Type of MOF | A | SA@Fe-BTC | SA@ZIF-8 |
| Dosage (mg) | B | 50 | 100 |
| Initial Concentration (mg/L) | C | 5 | 17 |

Table 3: The factorial design matrix and the experimental response results for MG removal efficiency.

| Run | A | B | C | Adsorption Capacity (mg/g) | % Removal | STD |
|-----|---|---|---|----------------------------|-----------|------|
| 1 | + | + | - | 1.035 | 96.479 | 1.67 |
| 2 | + | + | - | 1.054 | 93.142 | |
| 3 | + | - | - | 1.894 | 86.83 | |

| | | | | | | |
|----|---|---|---|-------|--------|------|
| 4 | + | - | - | 2.058 | 91.964 | 2.57 |
| 5 | + | - | + | 8.107 | 94.595 | 1.21 |
| 6 | + | - | + | 8.017 | 92.169 | |
| 7 | - | - | + | 3.774 | 44.084 | 2.23 |
| 8 | - | - | + | 3.211 | 39.631 | |
| 9 | - | + | + | 2.447 | 61.66 | 0.28 |
| 10 | - | + | + | 2.581 | 62.211 | |
| 11 | - | + | - | 0.774 | 70.387 | 1.78 |
| 12 | - | + | - | 0.833 | 73.942 | |
| 13 | + | + | + | 3.708 | 91.262 | 1.31 |
| 14 | + | + | + | 4.011 | 93.89 | |
| 15 | - | - | - | 1.627 | 71.903 | 3.80 |
| 16 | - | - | - | 1.447 | 64.286 | |

Figure 3 represents the cube plot which demonstrates the means of the response for the high and low levels of the variables used in the design. The plot revealed that the highest removal efficiency was achieved when using SA@ZIF-8 at higher dosages and lower initial concentrations, as indicated by the interaction effects and validation tests. Equations (3) was used to relate the removal efficiency of the MG dye with the process factors in coded terms as follows:

$$\text{Removal Efficiency} = 76.777 + 15.764 A + 3.594 B - 4.339 C - 2.443 A*B + 4.777 A*C + 1.224 B*C - 2.778A*B*C \quad (3)$$

These equations depict the effects of experimental factors and their interactions on the adsorption process of MG dye. The coefficients associated with each term indicate their impact on removal efficiency. For example, a positive coefficient for MOF dosage (B) suggests that an increase in dosage enhances removal efficiency, while a negative coefficient for the initial MG concentration (C) indicates that higher initial concentrations decrease efficiency.

Cube Plot (fitted means) for Removal Efficiency

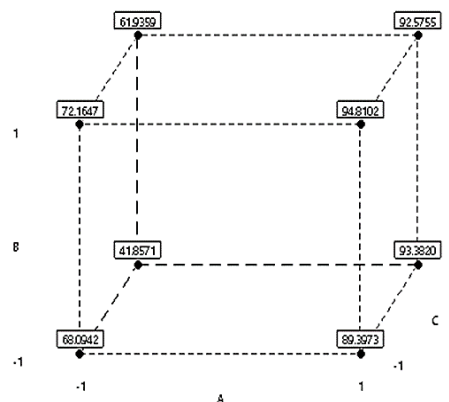


Figure 3: Cube plot for MG removal efficiency.

Additionally, interaction terms like $A*B$, $A*C$, $B*C$, and $A*B*C$ illustrate the combined effects of these factors. For instance, the negative coefficient for $A*B*C$ signifies a diminishing impact on removal efficiency when MOF type (A), dosage (B), and initial MG concentration (C) interact simultaneously. These equations provide a quantitative understanding of how these factors and their interactions influence the efficiency of malachite green removal in the adsorption process [16].

Table 4 presents the results of the 2^3 factorial design, outlining the main effects of the factors (MOF type, MOF dosage, and initial MG concentration), as well as the 2-way and 3-way interaction effects, along with their corresponding regression coefficients and standard deviations. Table 4 also includes the associated probabilities (P-values) used to determine the significance of these coefficients at a 95% confidence level. A P-value below 0.05 indicates that a coefficient is statistically significant. After reviewing ANOVA Table 4, it becomes clear that most coefficients are statistically significant, as indicated by their P-values being below 0.05. Notably, the analysis identified a positive effect for MG initial concentration, implying that higher initial concentrations led to increased adsorption efficiency. Conversely, MOF bead dosage had a negative effect, indicating that higher dosages had a diminishing impact on adsorption efficiency. Additionally, the type of MOF (with SA@ZIF-8) exhibited a positive effect, suggesting that it resulted in higher adsorption capacity. Significant 2-way and 3-way interactions further underscore the complexity of the relationship between these factors influencing the adsorption process.

Table 4. Analysis of variance (ANOVA) results for RE calculated using Minitab.

| Source | DF | Adj SS | Adj MS | F-Value | P-Value |
|--------------------|----|---------|---------|---------|---------|
| Model | 7 | 5092.22 | 727.46 | 82.51 | 0.001 |
| Linear | 3 | 4484.15 | 1494.72 | 169.53 | 0.001 |
| A | 1 | 3976.13 | 3976.13 | 450.97 | 0.000 |
| B | 1 | 206.72 | 206.72 | 23.45 | 0.001 |
| C | 1 | 301.30 | 301.30 | 34.17 | 0.000 |
| 2-Way Interactions | 3 | 484.55 | 161.52 | 18.32 | 0.001 |
| A*B | 1 | 95.48 | 95.48 | 10.83 | 0.011 |
| A*C | 1 | 365.11 | 365.11 | 41.41 | 0.000 |
| B*C | 1 | 23.96 | 23.96 | 2.72 | 0.138 |
| 3-Way Interactions | 1 | 123.52 | 123.52 | 14.01 | 0.006 |
| A*B*C | 1 | 123.52 | 123.52 | 14.01 | 0.006 |
| Error | 8 | 70.53 | 8.82 | | |
| Total | 15 | 5162.75 | | | |

The factorial design analysis, conducted using analysis of variance (ANOVA), revealed the primary influential factor to be the initial concentration of MG, followed by MOF bead dosage and the type of MOF bead, as depicted in the Pareto chart (Figure 4). Figure 4 reveals that the most influential factor was MOF type with a positive effect (SA@ZIF-8 shows better removal efficiency), followed by MG initial concentration with a negative effect and MOF bead dosage with a positive effect. Moreover, the variables that cross the reference line, which was found to be 2.31, are of high significance to the adsorption process and those that do not are insignificant. The present study revealed that A, B, and C and their interaction were considered significant for MG removal except for the 2-way interaction BC as it did not extend beyond 2.31.

The main effects display deviations from the average among the high and low values of each parameter. The intensity of effects that each parameter applies is displayed by the magnitude of the slope. In case of a positive slope, there will be an increase in the removal % for a high level of that parameter, and vice-versa. As shown in Figure 5, there are no horizontal lines connecting the mean for each parameter's levels, so there is a main effect for every variable.

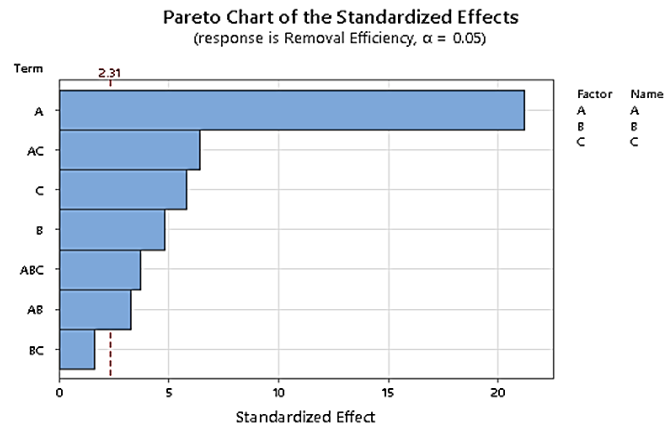


Figure 4. Pareto chart depicting the standardized effects on the removal efficiency.

There was a negative influence on the removal % for MG dyes due to the increase in the initial concentration (C). The MOF type (A) SA@ZIF-8 (+1) has significant effect on removal % whereas SA@Fe-BTC (-1).

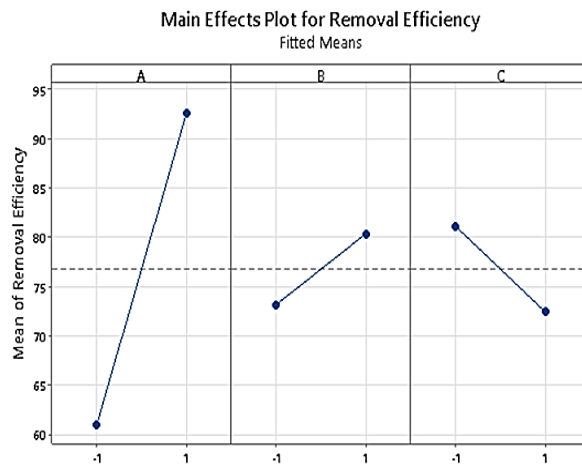


Figure 5. Illustrates the main effects plot depicting the impact of individual factors on the removal efficiency.

Figure 6 presents the interaction plots for 2-way interactions, revealing the combined effects of two parameters on the response variable. In the AB interaction, it is evident that SA@ZIF-8 efficiency remains largely unaffected by the dosage used, while SA@Fe-BTC exhibits higher removal efficiency with increased dosage. Notably, regardless of dosage levels, SA@ZIF-8 consistently achieves superior removal efficiency. Similarly, in the AC interaction, removal efficiency with SA@ZIF-8 remains consistent across various concentrations, whereas Fe-BTC demonstrates higher efficiency at lower initial MG concentrations. This outcome aligns with expectations, indicating that at

lower concentrations, MOF beads possess ample capacity to effectively remove dyes present in smaller quantities. Regarding B*C interactions, the results show that removal efficiency is higher at lower concentrations but decreases for higher dosages.

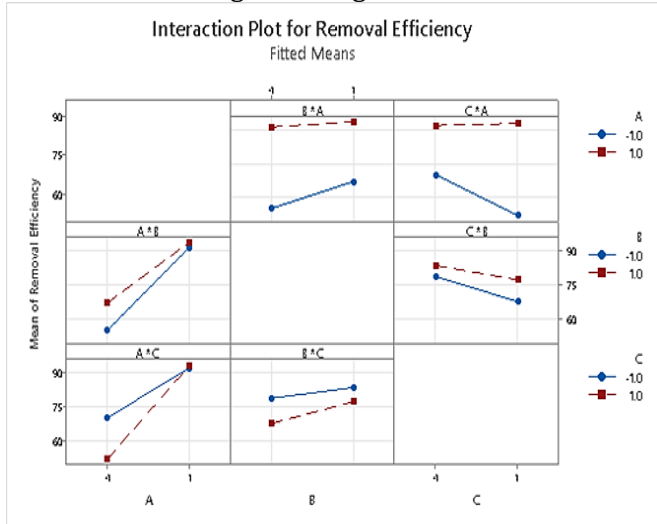


Figure 6. Interaction plot for removal efficiency.

The adequacy of the ANOVA model was verified by assessing normality, independence, and equality of variances, as illustrated in Figure 7. Barlett’s test was also conducted, yielding a P-value of 0.806, which is greater than the significance level of 0.05. Consequently, the null hypothesis could not be rejected, confirming the equality of variances. In summary, the highest removal efficiency was achieved when using SA@ZIF-8 at higher dosages and lower initial concentrations, as indicated by the interaction effects and validation tests.

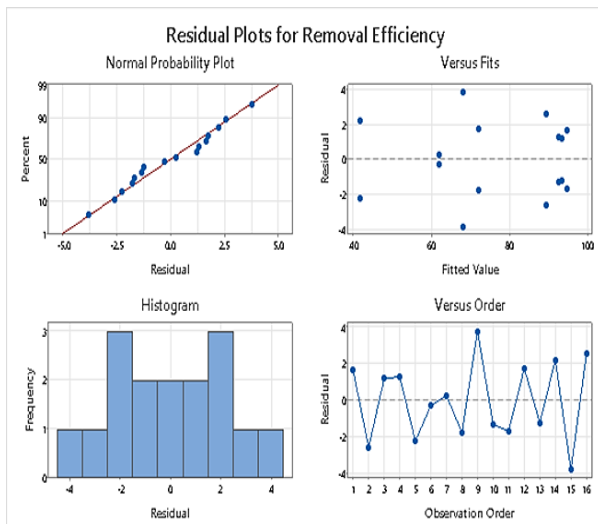


Figure 7. Residual plots for removal efficiency.

5. Conclusion

The study investigated the successful use of two metal-organic frameworks, SA@ZIF-8 and SA@Fe-BTC beads, for selectively removing malachite green dye from aqueous solutions. By thoroughly analyzing the effects of adsorbent dosage (50 to 100 mg) and initial MG concentration (7 mg/L to 15 mg/L) using a 2^3 full factorial design across 16 experiments (each repeated twice), the research provided significant insights into the adsorption capabilities of these metal-organic frameworks (MOFs). The experimental results indicated that the optimal removal of MG dye occurred when SA@ZIF-8 was administered at a dosage of 50 mg and an initial MG concentration of 17 mg/L. Through the use of sophisticated statistical techniques, including response surface methodology (RSM), t-tests, main effect analyses, interaction effect evaluations, and Pareto charts, the study not only identified the critical factors affecting the adsorption process but also quantified their individual and interactive impacts. The optimization process, guided by these analyses, led to the determination of precise conditions under which the highest removal efficiency of dyes from aqueous solutions could be achieved. Notably, the standout performance of the SA@ZIF-8 metal-organic framework emerged as a key highlight of the study. The results demonstrated that SA@ZIF-8 exhibited exceptional adsorption capabilities not only for MG dyes but potentially for a wide range of other dyes as well. These findings play a crucial role in advancing the field, providing clear directions for future research and facilitating the development of effective solutions for addressing water pollution challenges.

Acknowledgment

The authors gratefully acknowledge the financial support from the American University of Sharjah (FRG22-C-E27 and CEN-URG21-22).

References

- [1] R. Garg, R. Gupta, N. Singh, A. Bansal, “Characterization and performance evaluation of synthesized ZnO nanoflowers, nanorods, and their hybrid nanocomposites with graphene oxide for degradation of Orange G,” *Environ Sci Pollut Res Int*, vol. 28, no. 40, pp. 57009–57029, 2021.
- [2] G. Yin, Z. Sun, Y. Gao, S. Xu, “Preparation of expanded graphite for malachite green dye removal from aqueous solution,” *Microchemical Journal*, vol. 166, no. March, pp. 106190, 2021.

- [3] T. Zhang, X. Jin, G. Owens, and Z. Chen, "Remediation of malachite green in wastewater by ZIF-8@Fe/Ni nanoparticles based on adsorption and reduction," *J Colloid Interface Sci*, vol. 594, pp. 398–408, 2021.
- [4] S.B. Zadvarzi, M. Khavarpour, S.M. Vahdat, S.M. Baghbanian, A.S. Rad, "Synthesis of Fe₃O₄@chitosan@ZIF-8 towards removal of malachite green from aqueous solution: Theoretical and experimental studies," *Int J Biol Macromol*, vol. 168, pp. 428–441, 2021.
- [5] R. Garg and R. Sabouni, "Efficient removal of cationic dye using ZIF-8 based sodium alginate composite beads: Performance evaluation in batch and column systems," *Chemosphere*, vol. 342, Nov. 2023.
- [6] C. Wang, Q. Sun, L. Zhang, T. Su, Y. Yang, "Efficient removal of Cu(II) and Pb(II) from water by in situ synthesis of CS-ZIF-8 composite beads," *J Environ Chem Eng*, vol. 10, no. 3, pp. 107911, 2022.
- [7] S. Zhang, J. Wang, Y. Zhang, J. Ma, L. Huang, S. Yu, L. Chen, G. Song, M. Qiu, X. Wang, "Applications of water-stable metal-organic frameworks in the removal of water pollutants: A review," *Environ Pollut*, vol. 291, pp. 118076, 2021.
- [8] R. R. Ikreedeegh and M. Tahir, "A critical review in recent developments of metal-organic-frameworks (MOFs) with band engineering alteration for photocatalytic CO₂ reduction to solar fuels," *Journal of CO₂ Utilization*, vol. 43, pp. 101381, 2021.
- [9] A.A. Mohammadi, S. Moghanlo, M.S. Kazemi, S. Nazari, S.K. Ghadiri, H.N. Saleh, M. Sillanpää, "Comparative removal of hazardous cationic dyes by MOF-5 and modified graphene oxide," *Sci Rep*, vol. 12, no. 1, pp. 1–12, 2022.
- [10] YY. Si, Y. Li, G. Yang, S. Zhang, L. Yang, W. Dai, H. Wang, "Zeolitic imidazolate framework-8 for ratiometric fluorescence sensing tetracyclines in environmental water based on AIE effects," *Anal Chim Acta*, vol. 1199, pp. 339576, 2022.
- [11] Y. Song, N. Wang, L. Y. Yang, Y. G. Wang, D. Yu, and X. K. Ouyang, "Facile Fabrication of ZIF-8/Calcium Alginate Microparticles for Highly Efficient Adsorption of Pb(II) from Aqueous Solutions," *Ind Eng Chem Res*, vol. 58, no. 16, pp. 6394–6401, 2019.
- [12] M.A. Nazir, T. Najam, K. Shahzad, M.A. Wattoo, T. Hussain, M.K. Tufail, S.S.A. Shah, A. Rehman, "Heterointerface engineering of water stable ZIF-8@ZIF-67: Adsorption of rhodamine B from water," *Surfaces and Interfaces*, vol. 34, pp. 102324, 2022.
- [13] A.A. Castañeda-Ramírez, E. Rojas-García, R. López-Medina, D.C. García-Martínez, J. Nicolás- Antúnez, A.M. Maubert-Franco, "Magnetite nanoparticles into Fe-BTC MOF as adsorbent material for the remediation of metal (Cu(II), Pb(II), As(III) and Hg(II)) ions-contaminated water," *Catal Today*, vol. 394–396, pp. 94–102, 2022.
- [14] F. Hassani, A. Larki, M. Ghomi, N. Pourreza, "Gold nanoparticles embedded Fe-BTC (AuNPs@Fe-BTC) metal-organic framework as a fluorescence sensor for the selective detection of As(III) in contaminated waters," *Spectrochim Acta A Mol Biomol Spectrosc*, vol. 302, pp. 123104, 2023.
- [15] Y. Zhang, F. Li, W. Yuan, H. Yao, J. Zou, S. Liu, "Cadmium(II) adsorption with ZIF-8 nanocrystals of different morphology," *Microporous Mesoporous Mater.*, vol. 363, pp. 112837, 2024.
- [16] A. Karami, R. Shomal, R. Sabouni, M.H. Al-Sayah, A. Aidan, "Parametric Study of Methyl Orange Removal Using Metal-Organic Frameworks Based on Factorial Experimental Design Analysis," *Energies*, vol. 15, no. 13, 2022.